

Microwave-induced magnetooscillations and signatures of zero-resistance states in phonon-drag voltage in two-dimensional electron systems

A. D. Levin,¹ Z. S. Momtaz,¹ G. M. Gusev,¹ O. E. Raichev,² and A. K. Bakarov,^{3,4}

¹*Instituto de Física da Universidade de São Paulo, 135960-170, São Paulo, SP, Brazil*

²*Institute of Semiconductor Physics, NAS of Ukraine, Prospekt Nauki 41, 03028 Kyiv, Ukraine*

³*Institute of Semiconductor Physics, Novosibirsk 630090, Russia and*

⁴*Novosibirsk State University, Novosibirsk 630090, Russia*

(Dated: July 28, 2021)

We observe the phonon-drag voltage oscillations correlating with the resistance oscillations under microwave irradiation in a two-dimensional electron gas in perpendicular magnetic field. This phenomenon is explained by the influence of dissipative resistivity modified by microwaves on the phonon-drag voltage perpendicular to the phonon flux. When the lowest-order resistance minima evolve into zero-resistance states, the phonon-drag voltage demonstrates sharp features suggesting that current domains associated with these states can exist in the absence of external dc driving.

The microwave-induced resistance oscillations (MIRO) [1] and the related phenomenon of zero-resistance states [2] are observed in high-mobility two-dimensional (2D) electron systems placed in a relatively weak magnetic field B and subjected to microwave (MW) irradiation. The underlying physics of MIRO turned out to be unexpectedly rich, and its basic concepts have been applied to a variety of magnetotransport phenomena discovered recently [3]. The mechanisms of MIRO [3-9] originate from the scattering-assisted electron transitions between Landau levels due to absorption and emission of the MW radiation quanta by 2D electrons. Such processes strongly modify the energy distribution of electrons even in the case of overlapping Landau levels and lead to an oscillating contribution to electrical resistivity determined by the ratio of the radiation frequency ω to the cyclotron frequency ω_c . This physical picture is widely accepted [3], although alternative explanations of MIRO exist [10,11]. The theory successfully describes the period and phase of the magnetooscillations as well as the dependence of their amplitude on temperature and MW power.

The increase in MW power enhances the amplitude of MIRO and transforms the lower-order minima of magnetoresistance into the zero-resistance states (ZRS), the intervals of B where the dissipative resistance stays equal to zero. The theories developed for spatially homogeneous transport predict a negative resistivity in these intervals. Since the negative resistivity means that the homogeneous current distribution becomes unstable, it was suggested [12] that a pattern of current domains is formed in the sample. Indeed, in this regime a change in the current is accommodated by a shift of the domain walls without any voltage drop, so the resistance becomes zero. The experiments [13-16] support this concept.

In spite of attention to the MIRO and ZRS phenomena, experimental studies of the magnetotransport properties of 2D electrons under MW irradiation are almost entirely based on the measurements of electrical resistance or conductance under dc driving. An exception is the observation of MW-induced photovoltaic oscillations [17-19]. These oscillations occur in the samples with built-in spatial variation of electron density because the MW irradiation

strongly modifies the conductivity while leaving the diffusion coefficient unaffected [19]. Here we suggest that when temperature T varies across the sample, the MW irradiation creates conditions which allow one to observe, without any external dc driving, an oscillating thermoinduced voltage proportional to the resistance and closely resembling a MIRO signal.

To illustrate the basic idea, let us represent the current density as a sum of the drift current and the thermoelectric one [20], $\mathbf{j} = \hat{\sigma}\mathbf{E} - \hat{\beta}\nabla T$, where $\hat{\sigma}$ and $\hat{\beta}$ are the conductivity and thermoelectric tensors. In thermopower measurements, when $\mathbf{j} = 0$, the electric field $\mathbf{E} = \hat{\alpha}\nabla T$ is determined by the thermopower tensor $\hat{\alpha} = \hat{\rho}\hat{\beta}$, where $\hat{\rho} = (\hat{\sigma})^{-1}$ is the resistivity tensor. In the regime of classically strong magnetic fields relevant for high-mobility electrons, the longitudinal thermopower is $\alpha_{xx} = \rho_{xy}\beta_{yx} + \rho_{xx}\beta_{xx} \simeq \rho_{xy}\beta_{yx}$, since the second term is small as $(\omega_c\tau_{tr})^{-2}$, where τ_{tr} is the transport time. In the transverse thermopower, $\alpha_{xy} = \rho_{xy}\beta_{yy} + \rho_{xx}\beta_{xy}$, both terms are important. The main contribution to $\hat{\beta}$ in 2D systems comes from phonon drag mechanism [21-23], when electrons are driven by a frictional force between them and the phonons propagating along the temperature gradient. In these conditions, two terms in α_{xy} compensate each other [20] and $\alpha_{xy} = 0$ in the classical regime. Under MW irradiation the dissipative resistivity ρ_{xx} is strongly modified while the Hall one, ρ_{xy} , remains unchanged. The coefficients β_{yy} and β_{xy} are not modified by microwaves as strongly as ρ_{xx} [24]. Thus, the terms in α_{xy} no longer compensate each other, and the voltage developing in the direction perpendicular to the phonon flux should have an oscillating component proportional to the MW-induced part of dissipative resistivity.

In this Letter, we report experimental studies of phonon-drag voltage (PDV) in high-mobility 2D electron gas in four-terminal devices. We measure the dissipative resistance R_{xx} simultaneously with PDV and observe correlations of the PDV oscillations with MIRO under MW excitation. More important, we see sharp features in PDV corresponding to ZRS in R_{xx} , which apparently indicate that the ZRS domains can exist in the absence of

external dc driving. A theoretical consideration confirms the direct relation between PDV and resistance.

We have studied narrow (14 nm) quantum wells with electron density $n_s \simeq 10^{12} \text{ cm}^{-2}$ and a mobility $\mu = 2 \times 10^6 \text{ cm}^2/\text{Vs}$, at $T = 1.5 \text{ K}$. The 2D electron gas occupies a circular central part (diameter 1 mm) and four long (length $\simeq 5 \text{ mm}$, width 0.1 mm) arms ending with the voltage probes. The measurements have been carried out in a VTI cryostat with a waveguide to deliver MW irradiation (frequency range 110 to 170 GHz) down to the sample. The heater placed symmetrically between the arms 1 and 2 at a distance of 4.1 mm from the center (see Fig. 1) generates phonon flux. The voltages induced by this flux were measured by a lock-in method at the frequency of $2f_0 = 54 \text{ Hz}$ both in the longitudinal, V_{14} and V_{23} , and in the transverse, V_{12} (hot side) and V_{43} (cold side) configurations. Without powering the heater no photovoltage was observed. The thermovoltage increases linearly with heater power. We find the electron temperature near the heater and heat sink by the 2-probe measurements (contacts 1-2 and 3-4), exploiting the amplitude of the Shubnikov-de Haas (SdH) oscillation. The difference in the electron temperature between hot and cold sides is found $\Delta T \simeq 0.3 \text{ K}$ at the lattice temperature $T = 1.5 \text{ K}$. Several devices from the same wafer have been studied. The magnetoresistance (Fig. 1) was measured as a response V_{14} to the current injected through the contacts 2 and 3. The ZRS is seen at T below 4.2 K. Similar results are obtained for the other contacts.

The magnetooscillations of V_{23} and V_{12} , both with MW irradiation and without it (dark signal), are shown in Figs. 2 and 3. The transverse cold-side voltage V_{43} is much weaker than V_{12} , though shows the same periodicity as V_{12} . Both dark voltages V_{23} and V_{12} demonstrate acoustic magnetophonon oscillations whose period is determined by the ratio $2k_F s_\lambda / \omega_c$, where $k_F = \sqrt{2\pi n_s}$ is the Fermi wavenumber and s_λ is the sound velocity for phonon mode λ . These oscillations due to resonant phonon-assisted backscattering of electrons were observed previously [23]. The MW irradiation enhances both V_{12} and V_{23} by adding oscillating contributions odd in B . The positions of the peaks and minima of these PDV oscillations coincide with those of MIRO. The MW-induced contributions to V_{23} and V_{14} have opposite signs.

According to the general symmetry properties of thermoelectric coefficients, the odd in B voltages develop in the direction perpendicular to the temperature gradient or phonon flux. Thus, the odd in B behavior of V_{12} is expectable, while the appearance of odd in B contributions to V_{23} and V_{14} may look surprising. Explanation of this fact, however, is straightforward. The position of the heater between the long radial arms of the device (see Fig. 1) makes it clear that there is no homogeneous unidirectional phonon flux in the 2D area of the device. The phonons coming from the heater cross the arms attached to probes 1 and 2 in the directions perpendicular to these arms, so the voltages V_{23} and V_{14} , apart from the longitudinal (even in B) phonon-drag contributions, contain

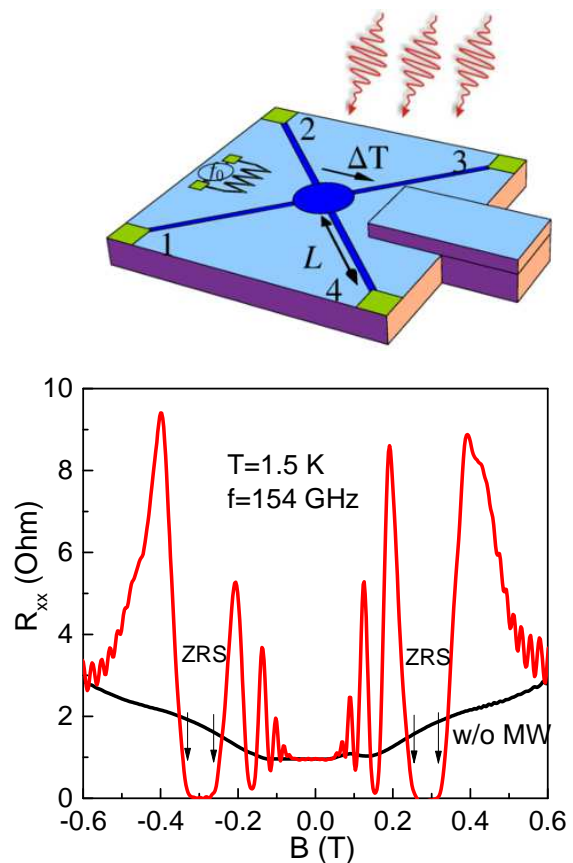


FIG. 1. (Color online) Sample geometry and longitudinal resistance without and with MW irradiation (154 GHz) as a function of magnetic field. Arrows show ZRS region.

significant transverse (odd in B) contributions. Since the phonons come to the arms 1 and 2 from different sides, the transverse contributions to V_{23} and V_{14} should have different signs, in agreement with our observation. Therefore, we identify the observed MW-induced voltages as a result of transverse phonon-drag effect (spatial redistribution of electrons in the direction perpendicular to the phonon flux) which is strongly enhanced because of the influence of microwaves on the resistance, as explained in the introduction.

To get more insight into the physics of the observed phenomenon, it is important to estimate the PDV theoretically. We believe that the drag in our experiment is mostly caused by high-energy ballistic phonons emitted from the heater in different directions [25], based on the following observations. First, the voltage V_{43} measured far away from the heater is much smaller than the voltage V_{12} , so the proximity to the heater is essential for the PDV signal. Second, the amplitude of magnetophonon oscillations of PDV in the absence of MW irradiation is much larger than expected for temperature $T = 1.5 \text{ K}$ in

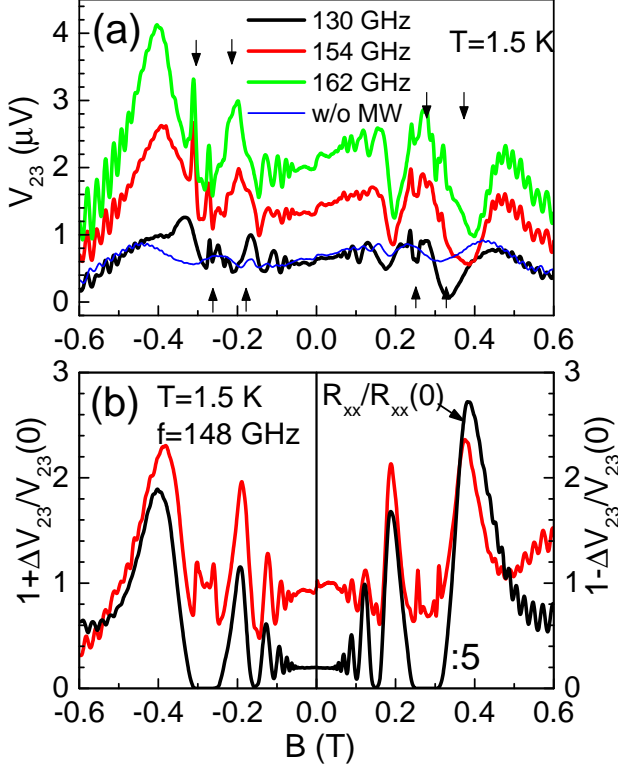


FIG. 2. (Color online) (a) Magnetic-field dependence of the longitudinal PDV V_{23} without and under MW irradiation for different microwave frequencies (shifted up for higher frequencies). Arrows show ZRS region. (b) PDV oscillations vs MIRO at 148 GHz. For clarity of the comparison, the sign of $\Delta V_{23} \equiv V_{23}(B) - V_{23}(0)$ is inverted at $B > 0$ and the resistance is scaled down by the factor of 5.

view of exponential suppression of backscattering in the Bloch-Gruneisen regime, $k_B T \ll 2\hbar k_F s_\lambda$, so the effective phonon temperature T_{ph} must be considerably higher than T . The ballistic phonon model is reliable because of large (1 mm) mean free path lengths of phonons in GaAs at low T [26]. Using the basic formalism for calculation of thermoelectric response in quantizing magnetic field [24] in application to this model [25], one may represent the PDV between the contacts i and j in the form

$$V_{ij} = \gamma_{ij}^L E_L + \gamma_{ij}^T E_T, \quad (1)$$

where E_L and E_T are the electric fields developing as phonon-drag responses to a homogeneous unidirectional phonon flux in the directions along and perpendicular to this flux, respectively, while the lengths γ_{ij}^L and γ_{ij}^T depend on the sample geometry. The PDV are formed by mixing of the longitudinal (even in B) and transverse

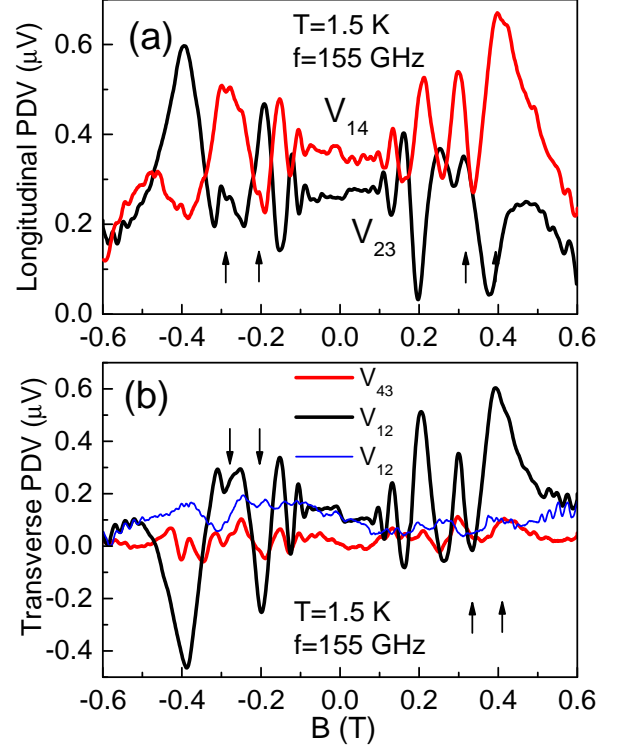


FIG. 3. (Color online) (a) Magnetic-field dependence of V_{23} and V_{14} under MW irradiation. The MW-induced contributions to these voltages have opposite signs. (b) Transverse PDV V_{12} (high-amplitude) and V_{43} (low-amplitude) under MW irradiation. Thin line: V_{12} without MW irradiation.

(odd in B) phonon-drag contributions described by the following expressions obtained in the regime of weak Landau quantization [25]:

$$E_L = F + 2d^2 G, \quad E_T = (2d^2 G - F \delta \rho_{xx} / \rho_0) / \omega_c \tau_{tr}, \quad (2)$$

where $\delta \rho_{xx} = \rho_{xx} - \rho_{xx}^{(0)}$, $\rho_0 = m/e^2 n_s \tau_{tr}$, $\rho_{xx}^{(0)} = \rho_0(1 + 2d^2)$ is the resistivity in the absence of MW irradiation, $d = \exp(-\pi/|\omega_c| \tau)$ the Dingle factor, τ the quantum lifetime of electrons and τ_{tr} the transport time. The quantity F does not depend on B while G is a function of B describing the magnetophonon oscillations of PDV [25]. In the absence of MW irradiation, $E_L \gg E_T$ in the relevant regime of classically strong magnetic fields, $|\omega_c| \tau_{tr} \gg 1$, so the dark PDV V_{23} is governed by E_L and is even in B . Under MW irradiation, E_T increases dramatically because of the large ratio $\delta \rho_{xx} / \rho_0$ and gives large, odd in B contributions to all measured PDV.

The theoretical plots of E_L and E_T for our sample are shown in Fig. 4. The effective temperature of ballistic

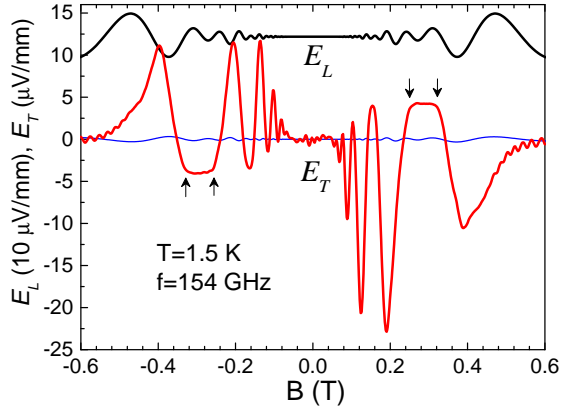


FIG. 4. (Color online) Calculated magnetic-field dependence of the fields E_L and E_T , the latter is plotted both with MW irradiation and without it (thin line). The function $\delta\rho_{xx}/\rho_0$ entering E_T is extracted from the experiment.

phonons, $T_{ph} \simeq 4$ K, is estimated from the amplitude of magnetophonon oscillations in V_{23} . The magnetic-field dependence of E_T shows a strong oscillating enhancement under MW irradiation. To plot it, we substituted the experimental dependence of $\delta\rho_{xx}/\rho_0$ into Eq. (2). Similar results are obtained using theoretical dependence of $\delta\rho_{xx}/\rho_0$ [7]. Our estimates of V_{23} and V_{12} based on the calculated E_L and E_T are in the general agreement with experiment (note that in Eq. (1) one should take into account that both γ_{ij}^L and γ_{ij}^T are small compared to the device size [25]). Therefore, the theory confirms that the observed MW-induced changes of the PDV are caused by the effect of microwaves on the dissipative resistance.

In the ZRS regions, the experimental PDV shows a

complex and diverse behavior that cannot be explained within the theory given above. Our observations reveal abrupt changes of the drag voltages in obvious correlation with the ZRS in R_{xx} , see Fig. 2 (b). Most often, the PDV, as a function of B , jumps at the beginning and at the end of the ZRS region, and more sharp features also appear within this region. We attribute this behavior to a transition from the homogeneous transport picture to the domain structure specific for the ZRS, since such a transition is accompanied with switching between different distributions of the electric field in the 2D plane [12,15]. We emphasize that in our experiment this transition occurs in the unusual conditions, when external dc driving is absent. Nevertheless, this fact rests within the general theoretical picture of ZRS [12], because the instability of the spatially homogeneous state is irrelevant to the presence of dc driving and requires only the negative conductivity created, for example, by MW irradiation. The resulting domains may carry electric currents, and the domain arrangement should provide zero currents through the contacts. The details of such domain structures are not clear and require further studies.

In summary, we observe MW-induced magnetooscillations of the phonon-drag voltage in GaAs quantum wells, correlating with the behavior of electrical resistance. The effect is described in terms of the sensitivity of transverse drag voltage to the dissipative resistivity modified by microwaves. The behavior of phonon-drag voltage in the zero resistance regime can be viewed as a signature of current domain state. Such MW-induced thermoelectric phenomena may show up in other 2D systems. The magnetothermoelectric measurements are therefore established as a tool to study the influence of MW radiation on the properties of 2D electrons and to gain complementary information about the MIRO and ZRS regime.

The financial support of this work by FAPESP, CNPq (Brazilian agencies) is acknowledged.

-
- [1] M. A. Zudov, R. R. Du, J. A. Simmons, and J. L. Reno, Phys. Rev. B **64**, 201311(R) (2001); P. D. Ye, L. W. Engel, D. C. Tsui, J. A. Simmons, J. R. Wendt, G. A. Vawter, and J. L. Reno, Appl. Phys. Lett. **79**, 2193 (2001).
 - [2] R. G. Mani, J. H. Smet, K. von Klitzing, V. Narayana-murti, W. B. Johnson, and V. Umansky, Nature **420**, 646 (2002); M. A. Zudov, R. R. Du, L. N. Pfeiffer, and K. W. West, Phys. Rev. Lett. **90**, 046807 (2003).
 - [3] I. A. Dmitriev, A. D. Mirlin, D. G. Polyakov, and M. A. Zudov, Rev. Mod. Phys. **84**, 1709 (2012).
 - [4] V. I. Ryzhii, R. A. Suris, and B. S. Shchamkhalova, Sov. Phys. Semicond. **20**, 1299 (1986).
 - [5] A. C. Durst, S. Sachdev, N. Read, and S. M. Girvin, Phys. Rev. Lett. **91**, 086803 (2003).
 - [6] M. G. Vavilov and I. L. Aleiner, Phys. Rev. B **69**, 035303 (2004).
 - [7] I. A. Dmitriev, M. G. Vavilov, I. L. Aleiner, A. D. Mirlin, and D. G. Polyakov, Phys. Rev. B **71**, 115316 (2005).
 - [8] I. A. Dmitriev, A. D. Mirlin, and D. G. Polyakov, Phys. Rev. B **75**, 245320 (2007).
 - [9] I. A. Dmitriev, M. Khodas, A. D. Mirlin, D. G. Polyakov, and M. G. Vavilov, Phys. Rev. B **80**, 165327 (2009).
 - [10] A. D. Chepelianskii and D. L. Shepelyansky, Phys. Rev. B **80**, 241308(R) (2009).
 - [11] S. A. Mikhailov, Phys. Rev. B **83**, 155303 (2011).
 - [12] A. V. Andreev, I. L. Aleiner, and A. J. Millis, Phys. Rev. Lett. **91**, 056803 (2003).
 - [13] R. L. Willett, L. N. Pfeiffer, and K. W. West, Phys. Rev. Lett. **93**, 026804 (2004).
 - [14] M. A. Zudov, R. R. Du, L. N. Pfeiffer, and K. W. West, Phys. Rev. Lett. **96**, 236804 (2006).
 - [15] S. I. Dorozhkin, L. Pfeiffer, K. West, K. von Klitzing, and J. H. Smet, Nature Phys. **7**, 336 (2011).
 - [16] A. T. Hatke, M. A. Zudov, J. D. Watson, and M. J. Manfra, Phys. Rev. B **85**, 121306(R) (2012).
 - [17] A. A. Bykov, JETP Lett. **87**, 233 (2008).
 - [18] S. I. Dorozhkin, I. V. Pechenezhskiy, L. N. Pfeiffer, K.

- W. West, V. Umansky, K. von Klitzing, and J. H. Smet, Phys. Rev. Lett. **102**, 036602 (2009).
- [19] I. A. Dmitriev, S. I. Dorozhkin, and A. D. Mirlin, Phys. Rev. B **80**, 125418 (2009).
- [20] R. Fletcher, Semicond. Sci. Technol. **14**, R1 (1999).
- [21] R. Fletcher, J. C. Maan, and G. Weimann, Phys. Rev. B **32**, 8477(R) (1985); R. Fletcher, J. C. Maan, K. Ploog, and G. Weimann, Phys. Rev. B **33**, 7122 (1986); R. Fletcher, P. T. Coleridge, and Y. Feng, Phys. Rev. B **52**, 2823 (1995).
- [22] C. Ruf, H. Obloh, B. Junge, E. Gmelin, K. Ploog, and G. Weimann, Phys. Rev. B **37**, 6377 (1988).
- [23] J. Zhang, S. K. Lyo, R. R. Du, J. A. Simmons, and J. L. Reno, Phys. Rev. Lett. **92**, 156802 (2004).
- [24] O. E. Raichev, Phys. Rev. B **91**, 235307 (2015).
- [25] See Supplemental Material, for details of calculation of phonon drag voltage within the model of ballistic phonon propagation.